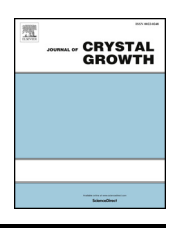
ELSEVIER

Contents lists available at ScienceDirect

Journal of Crystal Growth

journal homepage: www.elsevier.com/locate/jcrysgro



Growth and characterization of $In_xGa_{1-x}N$ (0 < x < 0.16) templates for controlled emissions from MQW



Mostafa Abdelhamid^{a,*}, J.G. Reynolds^b, N.A. El-Masry^b, S.M. Bedair^a

- ^a Department of Electrical and Computer Engineering, North Carolina State University, Raleigh, NC 27695, USA
- ^b Department of Materials Science and Engineering, North Carolina State University, Raleigh, NC 27695, USA

ARTICLE INFO

Communicated by M. Wevers

Keywords:

A3. InGaN relaxation

A3. Metal Organic Chemical Vapor Deposition (MOCVD)

A3. InGaN semibulk

A3. Multiple quantum wells (MQWs)

A1. High resolution X-ray diffraction (HRXRD)

B1. Nitrides

ABSTRACT

 $In_xGa_{1-x}N$ (0 < x < 0.16) templates were grown by Metal Organic Chemical Vapor Deposition (MOCVD) using the semibulk (SB) growth approach. We have studied the impact of different SB design parameters such as the number of (InGaN/GaN) periods, InGaN layer thickness (T), and the GaN substrate quality on the SB-template properties, and its degree of relaxation. SIMS characterization measured the variation of indium content (x) in the template, while photoluminescence reflected the indium content at the topmost layers of the SB template. X-ray diffraction techniques measured the average lattice parameters and degree of strain relaxation through the entire $In_xGa_{1-x}N$ SB-templates. The SB approach results in superior material quality relative to the bulk grown InGaN, mainly due to its ability to avoid the inclusion of indium-rich clusters and V-pits in the SB templates. The SB approach slows down the relaxation processes and templates as thick as 750 nm are not fully relaxed. We are reporting on methods to enhance the relaxation processes in $In_xGa_{1-x}N$ SB-templates. Finally, when $In_xGa_{1-x}N$ templates with $0 \le x \le 0.16$ are used as substrates for InGaN/GaN multiple quantum wells, the emission wavelength is shifted from blue to green by changing the indium content in the $In_xGa_{1-x}N$ SB-templates. To the best of our knowledge, the current results present the highest indium content reported in $In_xGa_{1-x}N$ SB-templates.

1. Introduction

Optical devices based on (InGaN/GaN) multiple quantum wells (MQWs) suffer from poor performance at long wavelengths and from efficiency droop, the phenomenon where the external quantum efficiency (EQE) drops at high current injection levels. Conventionally, In_xGa_{1-x}N/GaN light-emitting diodes (LEDs) are grown on GaN templates where the large lattice mismatch between GaN and InN (11%) leads to a high compressive strain in the QWs, especially for values of x necessary to emit in the green and red spectral regions [1]. The high compressive strain in the QW active region results in a blue shift in the band gap [2] and the large lattice mismatch limits the well width to a few nanometers to stay below the film critical layer thickness (CLT) [2,3]. In addition, the performance of LED structures grown along the caxis suffers from a large piezoelectric (PZ) polarization field. This PZ field has the beneficial effect of a redshift in the emission wavelength; however, it leads to the spatial separation between the electron and hole wave functions and a subsequent reduction in the quantum efficiency [1,2]. The relatively poor quality of $In_vGa_{1-v}N$ for high values of (y), coupled with compressive strain within the QWs' active region is believed to be the main reason for the "green gap" [1]. The compressive strain-induced piezoelectric field in the QWs can affect droop. However, recent experiments and theoretical modeling support Auger losses as the main cause of droop [4–6]. Auger recombination losses can be reduced by a reduction in carrier density, which can be achieved by increasing the QW thickness. Increasing the QW width requires reducing the compressive strain in these QWs. Therefore, it is desirable to reduce or eliminate the strain associated with the high lattice mismatch of GaN templates when growing high indium content QWs. Several approaches have been reported for the reduction of the PZ field and the droop in InGaN QWs [7–9].

Relaxed $In_xGa_{1-x}N$ templates with lattice constant close to that of the QWs represent the most desirable solution to eliminate the harmful effects of both biaxial strain and the PZ field. However, such templates are currently unavailable due to the difficulty in growing thick and relaxed $In_xGa_{1-x}N$ bulk films with good material quality, i.e. free from *V-shaped* defects and In metal inclusions with atomically smooth surfaces suitable for the growth of QWs with high indium content. Several attempts were reported using approaches such as a graded buffer, $ScAlMgO_4$ substrates, or thick $In_xGa_{1-x}N$ templates separated from

E-mail address: mabdelh2@ncsu.edu (M. Abdelhamid).

^{*} Corresponding author.

GaN films using the smart cut approach followed by wafer bonding [10–14]. These approaches produce templates with either low In content (x less than 0.06) in the ${\rm In}_x{\rm Ga}_{1-x}{\rm N}$ template, or poor properties [10–14]. ${\rm In}_y{\rm Ga}_{1-y}{\rm N}$ QWs with the indium content needed for green and red emission, typically with $y{\cong}0.2$, would be highly strained to such ${\rm In}_x{\rm Ga}_{1-x}{\rm N}$ templates. Other groups have inserted an (InGaN/GaN) superlattice (SL) between the GaN buffer layer and the LED QW structure. However, since the SL had low indium content and the InGaN layers are only a few nanometers thick, the SL remained fully strained to the GaN and does not relieve the compressive strain in the QW region. Albeit, improvements reported with these SLs do support better electron injection [15–17].

In this work, we present our effort to achieve strain relaxed $In_xGa_{1-x}N$ templates where $(0.08 \le x \le 0.16)$ based on the semibulk (SB) growth approach. We have developed these In_xGa_{1-x}N SB templates to minimize deleterious structural defects such as V-shaped defects (V-pits) [18], and indium metal inclusions that can occur in thick bulk InGaN films [19,20]. The semibulk templates are based on several cycles of InGaN/GaN layers grown on a thick GaN buffer. The growth starts with low temperature growth of an InGaN sublayer with thickness well below its CLT. A GaN interlayer (~1-2 nm thick) then caps the InGaN film. We then repeat this cycle, where one InGaN layer plus one GaN interlayer make up one period, for many periods to achieve the desired thickness of a strain relaxed or partially relaxed InxGa1-xN template. The GaN interlayers fill the V-pits generated in the InGaN film as the film relieves strain. The segregated indium metal at the surface of the growing InGaN film is systematically incorporated into the GaN interlayers, while the excess indium evaporates. This approach solves several of the main issues facing the bulk growth of InGaN templates. Previous preliminary efforts in developing InGaN SB-templates using the semibulk approach were limited to x[In] less than 0.1, by our group, or films with higher x[In] that were fully strained to the GaN template Γ19–221.

2. Experimental

In the current study, we investigated several growth parameters that affect the degree of strain relaxation and the film quality of $In_xGa_{1-x}N$ SB templates. These include the template's indium content (x), the thickness of the $In_xGa_{1-x}N$ layer (T), the number of (InGaN/GaN) periods (n), and the impact of the GaN buffer layer defect density on the

strain relaxation process. We will also show how the variations in the basic ${\rm In}_x{\rm Ga}_{1-x}{\rm N}$ SB structure, shown in Fig. 1, can enhance the strain relaxation process and reduce the growth time of the ${\rm In}_x{\rm Ga}_{1-x}{\rm N}$ SB-template to a practical value.

Our goal was to relieve strain on a period-by-period basis to increase the cumulative degree of strain relaxation as the number of periods increases.

All semibulk templates were grown on (0001) sapphire substrates by Metal Organic Chemical Vapor Deposition (MOCVD) at 350 torr with the precursors trimethylgallium (TMGa) and trimethylindium (TMIn) in a hydrogen and nitrogen ambient using ammonia for the group V constituent and silane for the n-type silicon dopant. The GaN nucleation layer was followed by 2 μ m of intrinsic GaN and another 2 μ m n-GaN. The reactor temperature was then reduced, and we introduced TMGa and TMIn to grow the $\ln_x \text{Ga}_{1-x} \text{N}$ layers at a growth rate of 11 nm/min followed by 2 nm interlayers of GaN at the same growth temperature followed by an anneal at $\sim 1000\,^{\circ}\text{C}$. We performed the growth of InGaN films and interlayers under nitrogen with only 2 sccm of H_2 flowing, the thicker GaN films were grown under a mixture of H_2 and N_2 . The indium content of the InGaN layers was controlled by changing the growth temperature (710–750 $^{\circ}\text{C}$). The InGaN SB-templates were capped with 10 nm of GaN.

We used Secondary Ion Mass Spectrometry (SIMS) to determine Indium content as a function of depth in the grown templates. Highresolution X-ray diffraction (HR-XRD) was used to determine the SB periodicity. InGaN SB film lattice parameters were estimated using a Philips X'Pert PRO MRD fitted with prefix module of a four-crystal Ge (220) monochromator using the Cu-K α_1 line and a graded multilayered parabolic mirror to diffract the incident beam. We have measured both the symmetric (0002), (0004), and the asymmetric ($10\overline{1}5$) reflections. The strained and relaxed lattice parameters and the periodic structure of the SB-templates are determined as discussed below. Atomic force microscopy (AFM) characterized the growth surfaces. Photoluminescence (PL) evaluated optical emission of the InGaN using a 325 nm He-Cd laser. To investigate the process of strain relaxation of the In_xGa_{1-x}N (SB) layers relative to the GaN substrate, high-resolution (1015) maps of the reciprocal lattice points (RSM) of the GaN template and (In_xGa_{1-x}N/GaN) SB layers were collected.

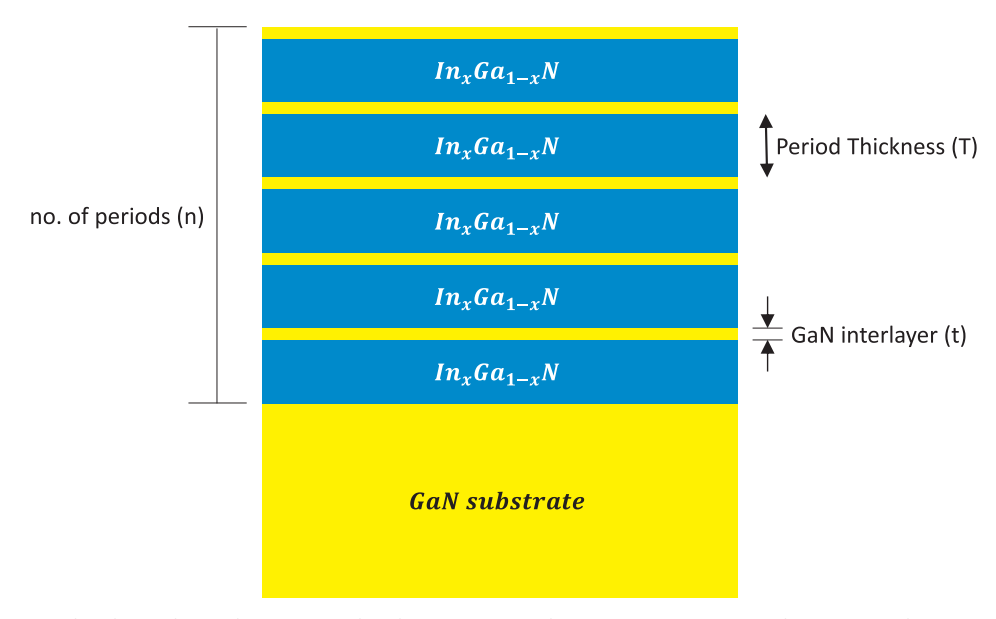


Fig. 1. Semibulk structure used in this study to achieve strain relaxed $In_xGa_{1-x}N$ template on GaN. Parameters to be investigated are (i) number of periods (n), (ii) width of the $In_xGa_{1-x}N$ period (T), (iii) indium content (x) of $In_xGa_{1-x}N$.

3. Results and discussion

The objective of this investigation is to generate InGaN SB templates with high degree of strain relaxation between the GaN substrate and the $In_xGa_{1-x}N$ layers, as shown in Fig. 1. There are several suggested mechanisms for strain relaxation in the hexagonal wurtzite films [12,23–28]. Examples are the formation of stacking faults, the inclusion of cubic crystal structures, 3D growth of indium-rich clusters, and V-shaped dislocation half-loops. It was recently suggested that V-pits formation during growth leads to strain relief [29,30]. It was reported from first principle calculations [29] that the formation of V-pits in InGaN films is energetically favorable because the indium-induced reduction in the surface energy on pit's sidewalls is much higher than on the (0 0 0 1) surface and these V-pits preferentially start at threading dislocation or indium-rich clusters [29–31].

To investigate the effect of the number of periods, three $\ln_x \text{Ga}_{1-x} \text{N}$ SB templates were grown targeting the same indium content (x), period thickness, $T=25\,\text{nm}$, and GaN interlayer thickness, $t=2\,\text{nm}$. The nominal n-type carrier concentration for the templates was $3\times 10^{18}\,\text{cm}^{-3}$ based on measurements of bulk GaN and InGaN films by van der Pawn Hall technique. The only variable between the three templates was the number of periods grown, n=20, 30, and 40 corresponding to thicknesses of 0.5, 0.75, and 1 μ m. These samples are referred to as 20P, 30P, and 40P, respectively. We chose the 25 nm thickness for the $\ln_x \text{Ga}_{1-x} \text{N}$ layers because it is below the critical layer thickness for the range of x[In] investigated in this current study [27].

We conducted SIMS measurement, shown in Fig. 2, on a 40P template to explore the general features of the $In_xGa_{1-x}N$ SB growth, the value of x, and the strain relaxation process. SIMS data show that the 40P SB template has three regions. The first region, close to the GaN substrate, consists of a few periods with constant indium content of $x \sim 0.066$. The second region starts after these few periods. Here the indium content (x) increases gradually in the growth direction from $x \sim 0.066$ to $x \sim 0.11$, this increase slows down after the 25th period. In the third region, the indium-content (x) levels off after the 35th period at $x \sim 0.12$. The oscillation in SIMS ion-count for indium between the InGaN layer and the GaN interlayer is strongly reduced in deeper periods. This is consistent with the expected spatial variation in the sputter crater depth with longer sputtering time. Nevertheless, the deeper periods are believed to have the same variation in indium content as present in the top layers. The relaxation takes place mainly in the second region; it is accompanied by an increase in the indium content as shown in Fig. 2. The third region has a constant indium

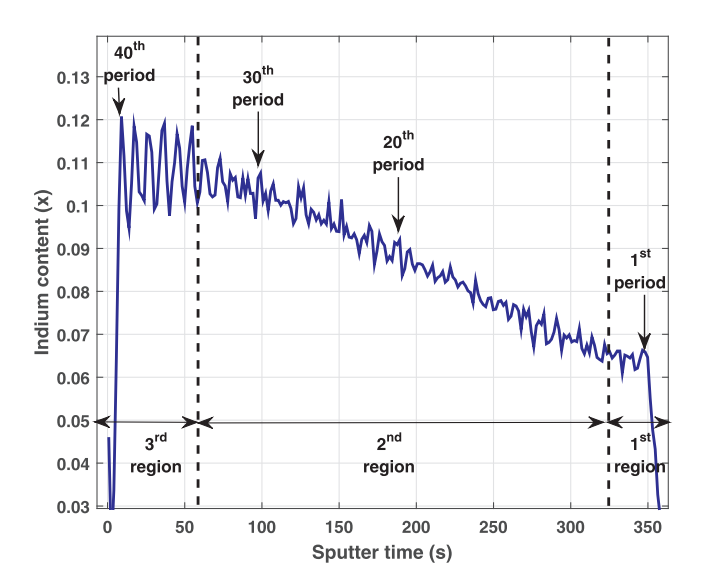


Fig. 2. SIMS depth profile of $In_xGa_{1-x}N$ SB sample 40P showing the variation of the indium content (x) with depth.

content of $x \sim 0.12$, and the InGaN SB film is close to being fully relaxed with a highly reduced residual strain. The thickness of the first and second regions depends on the template's indium content (x), $In_xGa_{1-x}N$ and GaN interlayer thicknesses, and $In_xGa_{1-x}N$ film's growth temperature. For samples with a lower number of periods such as 20P and 30P, SIMS measurements (not included here) have only shown the first two regions. Since samples 20P, 30P and 40P were all grown under the same conditions, we can use Fig. 2 to represent the variation of indium content (x) with the film layers thickness for the three templates. For the 20-period SB-template, the indium content (x) increases gradually from $x \sim 0.066$ at the GaN interface to $x \sim 0.092$ in the topmost 20th period, while for the 30-period SB-template, it increases gradually to $x \sim 0.1075$ in the 30th top period. The increased indium incorporation in the topmost layers as the film becomes more relaxed agrees with what others have previously reported for bulk InGaN growth [25,32-35]. Leyer et al. [35] showed an increase in indium content by a factor of 2-2.5 for bulk In_xGa_{1-x}N films with indium content of 0.15-0.2 as the films transition from fully strained to fully relaxed. This ratio is close to the 0.066 to 0.12 transition observed in sample 40P. The indium content at the top of samples 20P, 30P, and 40P can hence show the degree of strain relaxation in the SB templates.

We used high-resolution X-ray diffraction (HRXRD), symmetric and asymmetric rocking curves to characterize the ${\rm In}_x{\rm Ga}_{1-x}{\rm N}$ SB templates. Fig. 3 shows the (0004) and (10 $\overline{1}$ 5) x-ray scans for the 20P sample. The (0002) reflection, shown as an inset in Fig. 3, was used to confirm the InGaN SB template periodicity of 24 nm for all the SB samples.

The (0004) and the ($10\bar{1}5$) rocking curves of sample 20P shown in Fig. 3 show a single InGaN peak that reflects an average of the gradually increasing indium content from x \sim 0.066 to 0.092 as deduced from SIMS. However, when we increased the template thickness to 30 and 40 periods, the InGaN peak for both the (0004) and the ($10\bar{1}5$) reflections split into more than one peak. By comparing XRD of the 20P, 30P and 40P samples, the InGaN peak closest to the GaN peak was observed to be common to all three templates, as expected from Fig. 2 for the average indium content in the graded region. Therefore, we used a peak fitting program to determine the extra Bragg angles for the (0004) and the ($10\bar{1}5$) residing beneath the broad peak.

Fig. 4 shows the (0004) rocking curve of sample 40P which clearly reveals variable indium contents in the film. Guided by the SIMS data, we have assumed that the knee closer to the GaN peak is the initial $In_xGa_{1-x}N$ layers and the knee farther away represents the top layer that has a higher indium content. Two satellite peaks are also visible (n = +1) and n = -10 due to the periodic structure of the template.

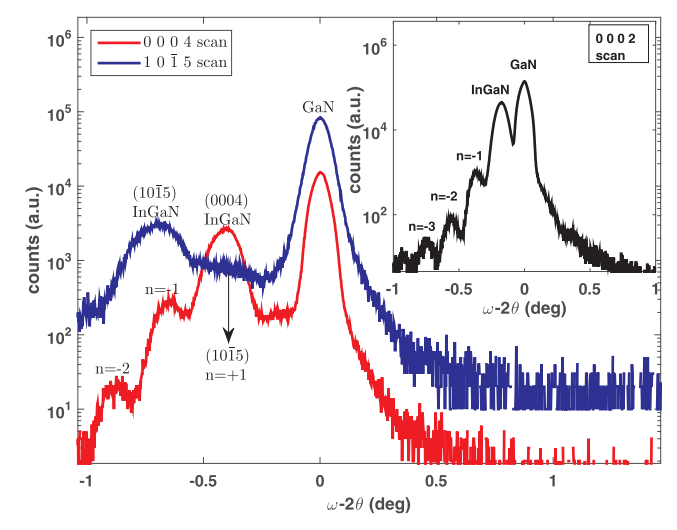


Fig. 3. Omega/2-Theta (0004) and $(10\bar{1}5)$ scans of 20-period semibulk template (20P). Figure Inset shows the (0002) reflection used to determine the period thickness.

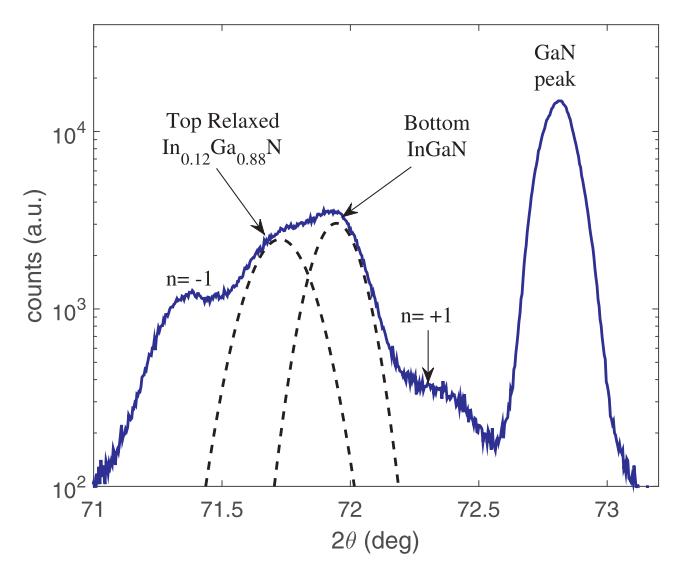


Fig. 4. (0 0 0 4) scan of 40-period $In_xGa_{1-x}N$ semibulk template (40P) showing the two distinct peaks "right and left knees" and their fitting to determine the indium content (x) and the degree of strain relaxation in the far bottom and top layers, respectively. The figure shows satellite peaks (n=+1 and n=-1) due to the periodic structure of the template.

The separation between the center of the InGaN peak and each of the two satellite peaks corresponds to a period of ~ 24 nm. Since the top 5 periods have shown an almost constant indium content from SIMS, we used the model developed by Schuster et al. [36] to calculate the indium content and degree of strain relaxation from the (0 0 0 4) and (10 $\overline{1}$ 5) scans. The indium content (x) of the top layers for 40P template from XRD was calculated to be 0.124 that agrees with the constant indium content of the top layers obtained from SIMS data (Fig. 2) and the degree of strain relaxation (R) was determined to be R \sim 93% [36].

The Reciprocal Space Mapping (RSM) technique is usually applied to characterize the composition of bulk InGaN films and the details of their degree of strain relaxation. However, in the current study, its use for InGaN SB-templates has served as much to indicate the limits of X-ray analysis as to provide a detailed analysis for two reasons. First, the SB has a periodic structure that results in satellite peaks that overlap with the main peaks and smear them out. Second, XRD techniques have a penetration depth of several micrometers, while the surface layer of the template of most interest is much thinner.

Representative reciprocal space maps (RSM) of $(10\bar{1}5)$ reflection of four $In_xGa_{1-x}N$ SB templates with 8, 13, 30 and 40 periods and total thicknesses of 160 nm, 260 nm, 750 nm, and 1000 nm are shown in Fig. 5(a-d), respectively. We grew the first two templates (8P and 13P) at different temperatures while the last two templates (30P and 40P) are grown at the same temperature as discussed earlier. The 8-period (8P) template, Fig. 5(a), is fully strained to the GaN substrate with indium content $x \sim 0.095$. The reciprocal lattice point (RLP), n = 0, broadens because of a slight increase in both indium content and strain relaxation. The main peak and the satellite spots are aligned slightly off the vertical pseudomorphic R = 0 line. This indicates that the 160 nm thick $In_xGa_{1-x}N$ SB-template with $x \sim 0.095$, which is several times thicker than the CLT, is almost fully strained. This data is consistent with previous SB work [22], where $In_{0.15}Ga_{0.85}N$ with a total thickness of 120 nm was reported to be fully strained from RSM.

As the number of periods is increased to 13P, Fig. 5(b), the indium content changes from the fully strained value, of $x\sim0.14$ to higher values as the film relaxes with increasing film thickness. Thus, the RLPs are elongated because of both composition and strain gradients as shown in Fig. 5(b). Data in Fig. 5(b) indicate that the indium content (x) varies from 0.14 to 0.16 with the topmost periods being $\sim\!50\%$ relaxed. The satellite peaks corresponding to n=+1 and n=-1 shown in

Fig. 5(b) result from the periodic SB structure as shown in Fig. 1. We calculated the period thickness $T=(0.5\lambda/\sqrt{\Delta Q_x^2+\Delta Q_z^2})$ from the separation between two successive satellite peaks in the RSM and it matches the period deduced from the HRXRD (0002) scan. Results shown in Fig. 5(b) demonstrate the ability to have SB templates with indium content x \sim 0.16 that is desirable reduce strain in QW emitting in the green region.

As the number of periods increases to 30 and 40, Fig. 5(c) and (d), the RLP of the n = -1 satellite merges with the RLP originated from n = 0 peak. The first few periods remain fully strained and coherent to the GaN substrate with $x \sim 0.07$. The results are consistent with the SIMS data for the 40P template. With increasing SB thickness, the maximum of the RLP progressively shifts from a fully strained pseudomorphic film towards the fully relaxed line with R = 100%. There is a progressive shift in the RLP towards iso-composition lines with higher indium content consistent with the SIMS results. Additionally, in the 40P case, the RLP satellite peaks for n = -1, n = 1 and 2 are merging with the n = 0 peak and smear the whole RLP to one very broad (10 $\bar{1}$ 5) reflection. This makes it difficult to determine the degree of strain relaxation quantitatively for samples 30P and 40P. The highly relaxed top layer in sample 40P is not clearly observed as a separate peak in Fig. 5(d), perhaps due to low intensity from only six periods relative to the strong broad peak arising from the 34 periods buried layers with graded composition.

The XRD data, shown in Figs. 4 and 5, reflect the variations in the lattice parameters through the entire ${\rm In}_x{\rm Ga_1}_{-x}{\rm N}$ SB film thickness. This results in a broad (10 $\bar{1}$ 5) rocking curve and an RSM that reflects both a high-intensity peak for the bottom-embedded thick layers and another less intense peak for the topmost thin more strain-relaxed layers. This difficulty of identifying thin relaxed film by RSM was also reported earlier [34].

For the use of ${\rm In}_x{\rm Ga}_{1-x}{\rm N}$ SB templates as substrates for MQW structures, two parameters are of interest: the degree of strain relaxation and the lattice constant of *the topmost layer*. In the following, we will use the PL technique along with SIMS measurement to identify the above two parameters for the topmost layers of the SB structure. The PL technique uses a HeCd laser that is mainly absorbed after about 100 nm in GaN. Thus, the PL signal originates from electron-hole recombination resulting from the topmost layers.

The PL emission spectra of the three samples (20P, 30P, and 40P), shown in Fig. 6, shows a shift in the emission wavelength from 414 nm to 429 nm to 443 nm for 20P, 30P and 40P templates, respectively. The 30 nm red shift in emission wavelength in the $In_xGa_{1-x}N$ SB template is evidence that the InGaN band gap (Eg) decreases as the number of periods increase where both strain relaxation and composition grading are involved. We also observe a gradual decrease in emission intensity that reflects a gradual degradation in crystal quality.

We have compared the band gaps from PL data for 20P, 30P and 40P templates shown in Fig. 6 with the band gap data for strained and relaxed bulk InGaN [37,38]. We can express the band gap of strained InGaN film as:

$$E_g(In_xGa_{1-x}N) = E_g^{Relaxed}(InGaN) + \Delta E_g^{strain}$$

$$= (1-x)E_g^{GaN} + xE_g^{InGaN} - b_{InGaN}x(1-x)$$

$$+ [-14.22\varepsilon_{xx} - 51.603\varepsilon_{xx}^2]$$
 (1)

where $E_g^{GaN}=3.4eV$, $E_g^{InGaN}=0.7eV$, bowing parameter $b_{InGaN}=2.5eV$, and ε_{xx} is the strain in the basal plane. The shift in the band gaps of the ${\rm In}_x{\rm Ga}_{1-x}{\rm N}$ SB templates, for a given indium content; relative to the relaxed InGaN bulk band gap is related to the residual strain in the top layers of the templates.

SIMS data in Fig. 2 show that the 20P sample has an indium content of $x \sim 0.092$ for the topmost periods while sample 30P has an indium content of $x \sim 0.1075$. Knowing the band gap value from PL measurements, we can deduce the strain value in the film from Eq. (1). Then the lattice parameter a_{InGaN} of the topmost layers is calculated using the

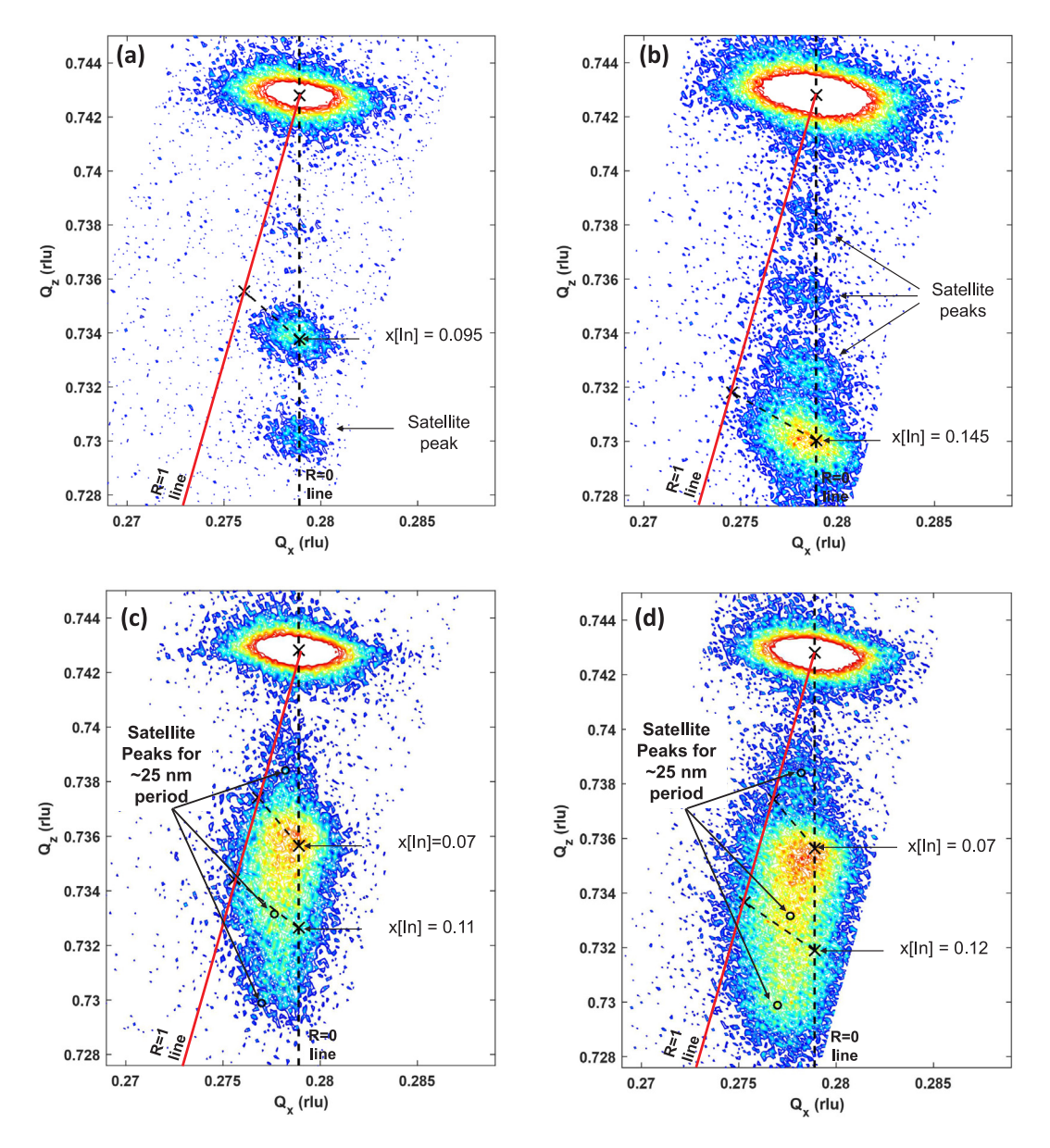


Fig. 5. (1015) reciprocal space map of (a) 8-period SB, (b) 13-period SB, (c) 30-period SB, (d) 40-period SB templates. Satellite peaks here indicate the periodicity of the SB structure.

deduced strain value:

$$a_{InGaN} = a_{InGaN}^{relaxed} (1 + \varepsilon_{xx})$$
 (2)

where $a_{mGaN}^{relaxed}$ is the lattice parameter of relaxed InGaN film and is calculated from Vegard's law as a function of indium content (x):

$$a_{InGaN}^{relaxed}(x) = xa_{InN} + (1 - x)a_{GaN} - b_{InGaN}^*x(1 - x)$$
 (3)

where $a_{InN}=3.538$ Å, $a_{GaN}=3.1893$ Å, and bowing parameter $b_{InGaN}^*=0.003$ Å [39]. The degree of strain relaxation $\{R=[a_{InGaN}-a_{GaN}]/[a_{InGaN}^{relaxed}-a_{GaN}]\}$ is then determined.

Thus, for the 20P InGaN SB template, the PL emission at 414 nm is mainly because of carrier recombination within the top layers with $x\sim 0.092$ as shown in SIMS data. This results in a degree of relaxation of about R=62%. For the 30P sample with $x\sim 0.1075$ indium in the top layers, the PL emission is at 429 nm which results in a degree of relaxation of R=83%. Thus, our $In_xGa_{1-x}N$ SB templates as thick as 750 nm are not fully relaxed, which is a completely unexpected result. As for 40P sample, both XRD and SIMS show that the indium content is about $x\sim 0.12$ in the top periods where PL emission is at 443 nm

corresponds to almost full strain relaxation. Similar degree of strain relaxation values 40P template was deduced from HRXRD shown in Fig. 4. However, the PL data gives about 10% greater relaxation than the X-ray measurements.

To enhance the strain relaxation process in the $In_xGa_{1-x}N$ SB-templates without growing 40 periods, which takes 4–5 h, a SB structure with identical indium content to sample 40P was grown with varying the $In_xGa_{1-x}N$ layer thickness (T). The structure consisted of 14 periods of T = 25 nm (InGaN/GaN) followed by six periods of gradually increasing InGaN layer thickness from 25 nm to 37.5 nm thickness of the topmost period. The total thickness of the template was 547 nm comparable to that of the 20P sample. The rationale for investigating this structure was to determine whether residual strain in the growing InGaN SB-templates decreases as the InGaN layer thickness increases. The (0002) reflection for the structure confirms the 25 nm periodicity of the bottom 14 periods and the high quality of interfaces in the SB. The PL emission of this template is shown in Fig. 7(b), it shows a 443 nm emission which is comparable to that of sample 40P indicating that a 20-period template with gradually increasing InGaN thickness is more

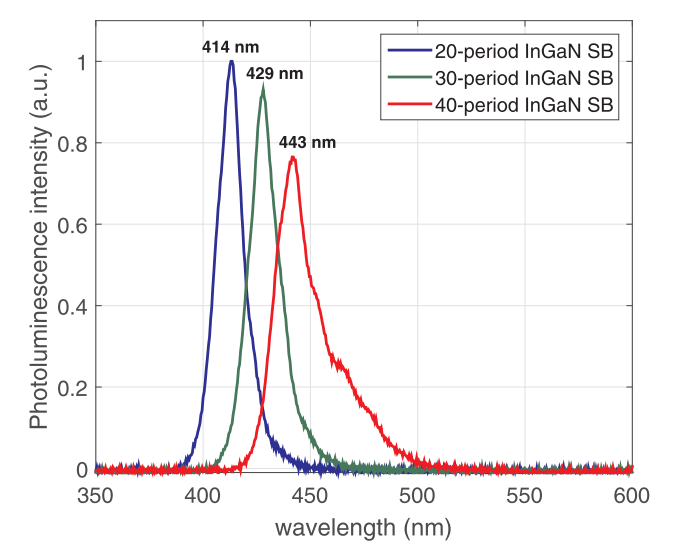


Fig. 6. Comparison of PL emission for 20, 30 and 40-period SB templates grown at the same conditions.

relaxed as compared to sample 20P that has a fixed period thickness. This result indicates that increasing the InGaN layer thickness enhances the strain relaxation process. Most importantly, the result represents the potential of growing relaxed templates with good optical properties in half the growth time compared to sample 40P. The RSM results for this template are shown in Fig. 7(a), however, as discussed earlier it is difficult to determine quantitively the degree of relaxation for the thin topmost layer from RSM.

Finally, we investigated the impact of the substrate dislocation density on the elastic strain relaxation process in InGaN SB templates. We compare two GaN substrates: first is our grown GaN layer with threading dislocation densities (TDD) of mid to high $10^9\,\mathrm{cm}^{-2}$. The second is a commercial GaN on sapphire substrate with TDD of mid to low $10^8\,\mathrm{cm}^{-2}$. An InGaN SB template with 30 periods and T = 25 nm was grown on the low TDD substrate. The growth conditions were the same as sample 30P that was grown on our GaN that has an order of magnitude higher TDD. Fig. 8(a) shows that the PL emission from the SB template grown on low TDD substrate is shorter than that on the one with higher TDD. The RSM results from this SB template are shown in Fig. 8(b) and can be compared with those shown in Fig. 5(c) for sample

30P that was grown on high TDD substrate. The results from Fig. 8 indicate that high TDD in the substrate enhances strain relaxation in the $In_xGa_{1-x}N$ SB templates while on low TDD substrate pseudomorphic growth is kept up to higher thickness. RSM in Fig. 8(b) shows also that the indium content starts with strained $x\sim0.07$ close to the GaN substarte and it increases only to $x\sim0.085$ in the top layers. The top layers have a peak intensity that lies on the $x\sim0.085$ line and corresponds to a degree of strain relaxation close to R=13%. This indium content and strain relaxation value agree with the 403 nm emission from PL in Fig. 8a. These results are consistent with the previous studies reported by Ju et al. [34] showing that high dislocation densities reduce the $In_xGa_{1-x}N$ critical layer thickness and enhance both surface roughness and strain relaxation.

We used AFM to study surface roughness of the InGaN SB templates. Data for AFM (RMS) roughness for $1\times 1~\mu m^2$ areas are summarized in Table 1 along with the degree of strain relaxation as deduced from HRXRD. We have also included AFM data from a bulk grown 60 nm In $_{0.075}\text{Ga}_{0.925}\text{N}$ for comparison. Bulk samples that are several hundred nanometers thick have roughness larger than 100 nm.

From Table 1, the SB approach results in improved surface quality relative to bulk grown templates. Fig. 9 shows AFM images of some samples listed in Table 1. The surface roughness increases with the increasing number of periods and increasing indium content. It also appears from these limited data that the sample surface is rougher when the template thickness approaches the regions of constant film composition, i.e. high levels of strain relaxation. It may be difficult to deduce from these limited data the growth mode of the top layer without extensive TEM studies that are underway. However, templates with 20 periods, 500 nm thick with indium content close to $x \sim 0.1$, have decent surface morphology. The best AFM surface roughness of 0.94 nm is obtained when substrates with low defect density are used. The SB approach results in highly improved surface roughness as compared to bulk grown InGaN films. We believe that partially relaxed InGaN SB templates are device quality and offer new substrates for InGaN based QW devices. However, more work is underway to optimize the SB growth parameters to improve further the quality of these templates particularly those with high values of x.

The strain relaxation mechanism in SB samples is not the subject of this paper and requires detailed TEM investigations. However, we will discuss some similarities and differences in the growth of bulk and InGaN SB templates based on our past extensive experience in the growth of InGaN films.

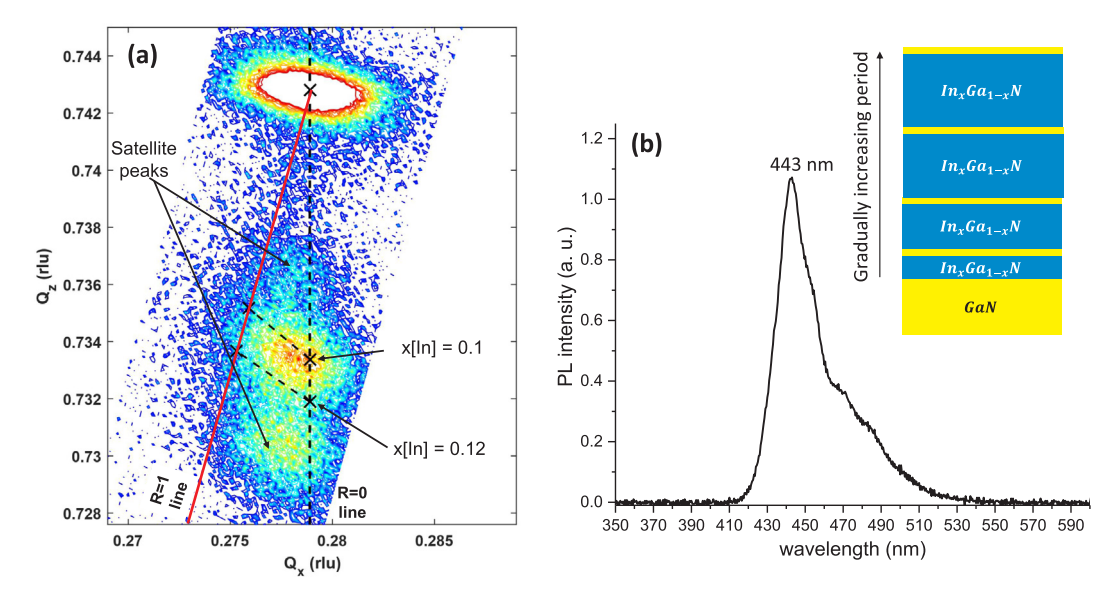


Fig. 7. (a) (1015) reciprocal space map of 20-period SB with gradually increasing period thickness from 25 nm to 37.5 nm, (b) PL emission of the structure with the inset showing the schematic.

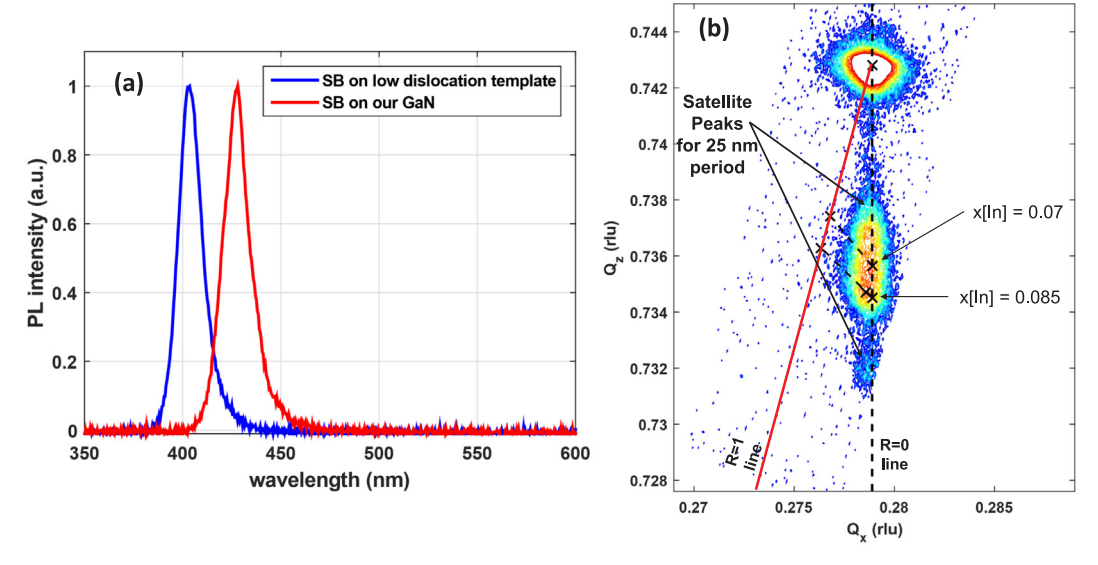


Fig. 8. (a) Normalized PL emission of 30-period SB template grown on our GaN buffer versus a template grown on a low dislocation GaN template. (b) (1015) reciprocal space map of 30-period SB sample grown on low dislocation GaN template.

Table 1 Summary of $1 \times 1 \mu m^2$ roughness of different samples measured by AFM.

Sample	1 μm RMS Roughness	Degree of strain relaxation
60 nm Bulk <i>In</i> _{0.075} <i>Ga</i> _{0.925} <i>N</i>	48 nm	Fully relaxed
20-period In _{0.07} Ga _{0.93} N SB	1.40 nm	~ 40%
20-period In _{0.085} Ga _{0.915} N SB	2.65 nm	~62%
30-period In _{0.11} Ga _{0.89} N SB	4.55 nm	~83%
30-period In _{0.12} Ga _{0.88} N SB on low TDD substrate	0.943 nm	~13%
40-period $In_{0.12}Ga_{0.88}N$ SB	6.51 nm	~90%

In the following discussion, we compare our earlier results [26] obtained from five separate InGaN bulk grown samples (69 nm, 200 nm, 400 nm, 520 nm and 730 nm thick) with the InGaN SB templates: 20P, 30P, and 40P, presented in the current study. Both bulk and SB films have the same starting indium content of $x \sim 0.07$ to allow for a fair comparison. Both bulk and SB films start with a highly strained layer coherent to the GaN substrate for about ~ 70 nm as shown in SIMS Fig. 2 for the SB templates and as reported from TEM results for the bulk samples from reference [26].

For bulk-grown thicker InGaN films, the PL emission and XRD show broad, multiple peaks, and the sample surface starts to undulate while thick samples had a saw-like surface with a roughness of over 100 nm. TEM of these bulk samples showed stacking faults, poly-type like area, and a high density of planar defects. The indium content in both samples (bulk and SB templates) increases from $x \sim 0.07$ at the GaN interface to $x \sim 0.094$ for 500 nm thick samples. The 750 nm bulk InGaN sample is fully relaxed and the RSM showed two peaks for the fully strained and fully relaxed samples [26]. A possible growth mode for the InGaN films is that the initial strained layer matches the underlying GaN and rejects indium-atoms, which segregate on the sample surface causing indium-rich clusters. Such excess indium-rich clusters initiate the formation of defects and V-pits. Therefore, for bulk growth as soon as the thickness of the InGaN layer exceeds the CLT; defects appear, and these indium-rich clusters enhance the strain relaxation processes. Leyer et al. [35] have also argued that the increased surface roughness in relaxed bulk InGaN films can offer more stable indium incorporation sites compared to relatively smooth surfaces. However, in the SB growth approach, these excess indium atoms that segregate to the surface either are accommodated in the GaN interlayers or are evaporated when the GaN interlayer is annealed at ~1000 °C after each period. The absence of these indium-rich clusters and the decreased surface roughness impede the strain relaxation process. This allows films with 750 nm thickness to be partially relaxed with few nanometers surface roughness rather than 100 nm roughness observed in bulk InGaN. A detailed TEM study is underway to reveal the strain relaxation mechanism in the InGaN SB templates.

4. Quantum well structure on InGaN templates

We have used In_xGa_{1-x}N SB templates as substrates for the growth of (InGaN/GaN) MQW active layers. First, (In_vGa_{1-v}N/GaN) MQWs with 2.5 nm thick wells and 6 nm barriers were grown on GaN as a reference sample, then the same MQWs were grown under the same growth conditions on three different In_xGa_{1-x}N SB templates having different indium content in the SB. These templates are partially relaxed and were grown at temperatures targeting an indium content (x) at the topmost layer of these templates of 0.09, 0.12, and 0.14 respectively. Fig. 10 summarizes the PL peak emission wavelengths of these MQWs versus the growth temperature of the In_xGa_{1-x}N SB templates in comparison with the reference sample that was grown on GaN. The emission wavelength for each sample is shifted from blue (MQW on GaN) to green (MQW on SB template with $x \sim 0.14$) as a function of indium content in the In_xGa_{1-x}N SB template. Thus, the composition of the $In_xGa_{1-x}N$ SB template influences the emission wavelength of the MQW stack. This is accompanied by a reduction in the QW optical transition energy as the lattice mismatch between the InGaN quantum well and In_xGa_{1-x}N SB template is reduced with increasing indium content in the template. The redshift of 5, 15, and 37 nm in the PL emission wavelength for templates with $x \sim 0.9$, 0.12, and 0.14 relative to that of the conventional device can be attributed to changes in the indium content (y) of the InyGa1-yN QWs, and reduction in compressive strain and the PZ field in the MQW [2]. It is difficult to determine which of these parameters are responsible for this redshift in the PL emission because of the uncertainty in the degree of strain relaxation. Thus, the data in Fig. 10 shows that the $In_xGa_{1-x}N$ SB-templates are device quality without trying to deduce quantitative values. This is one of the major goals of our current work.

5. Summary

We have developed and characterized relaxed and partially relaxed $In_xGa_{1-x}N$ SB-templates (0 < x < 0.16) to use as substrates for strain-

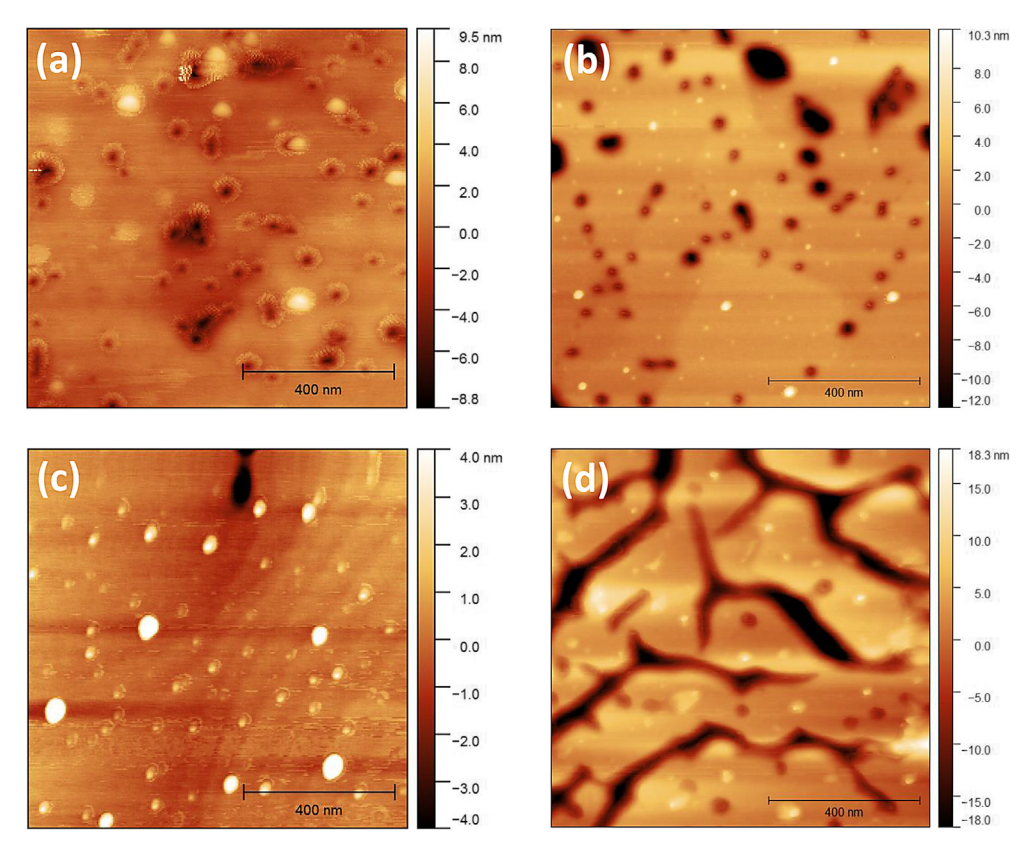


Fig. 9. AFM images of a 1 μ m \times 1 μ m area of (a) 20-period $In_{0.07}Ga_{0.93}N$ SB, (b) 20-period $In_{0.085}Ga_{0.915}N$ SB, (c) 30-period InGaN SB on low dislocation template, (d) 40-period $In_{0.12}Ga_{0.88}N$ SB.

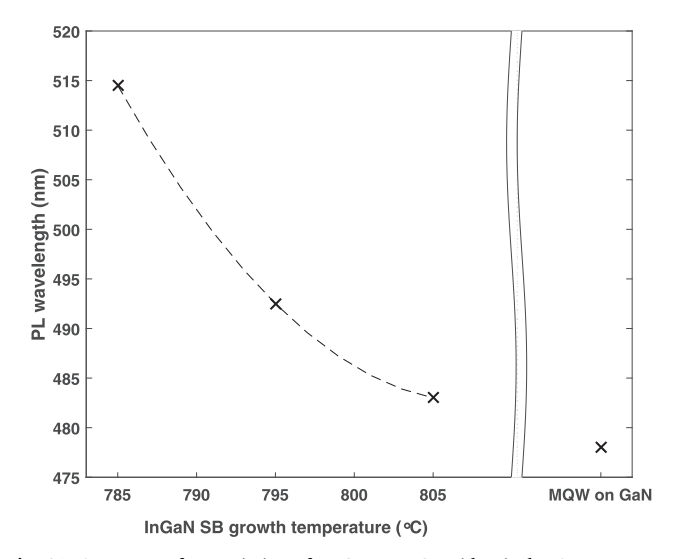


Fig. 10. Summary of PL emission of $In_yGa_{1-y}N/GaN$ identical MQW structures grown on $In_xGa_{1-x}N$ SB templates of different Indium content (x) in the template by varying the growth temperature of the SB.

free InGaN based MQW structures. In the SB growth approach, we insert thin GaN interlayers between the InGaN layers. We studied the impact of the number of periods, indium content (x), and the $\rm In_x Ga_{1-x}N$ layer thickness on the degree of strain relaxation of the $\rm In_x Ga_{1-x}N$ SB-templates using SIMS, HRXRD, RSM, PL, and AFM. We found that HRXRD reflects the average lattice parameters and the strain relaxation through the entire SB template while RSM results were shown to be difficult to evaluate for periodic SB structures. SIMS and PL data reflects the state of strain relaxation of the topmost layer in the SB structure. We also report that a high TDD in the GaN buffer layer

enhances the strain relaxation in the InGaN SB templates. We report methods to enhance the strain relaxation process by changing the template's InGaN layers thickness T.

The SB approach results in superior material quality relative to the bulk grown InGaN, mainly due to its ability to avoid the inclusion of indium-rich clusters. This results in templates with smooth surfaces and excellent optical properties. The SB growth approach slows down the strain relaxation processes and templates as thick as 750 nm are not fully relaxed. Also, the value of x in $\ln_x Ga_{1-x}N$ SB film changes over the thickness of 1000 nm from x \sim 0.7 close to the substrate to x \sim 0.12 at the template surface.

Finally, ${\rm In_yGa_{1-y}N/GaN}$ multiple quantum wells (MQWs) were grown and tested on our ${\rm In_xGa_{1-x}N}$ SB-templates with $0 \le x \le 0.16$. The emission wavelength for the same MQW is shifted from blue to green by changing the value of x in the template. To the best of our knowledge, the current results present the highest Indium content reported in an ${\rm In_xGa_{1-x}N}$ SB template grown by MOCVD.

Acknowledgment

We would like to acknowledge the technical discussions with Dr. Lew Reynolds, Dr. P. Colter, Dr. D. Van Den Broeck, and Thomas Leonard. We would also like to acknowledge C. Zhou with NCSU Analytical Instrumentation Facility for the SIMS measurements. This work is supported by National Science Foundation grants: ECCS-1407772 and ECCS-1833323.

References

- [1] S. Saito, R. Hashimoto, J. Hwang, S. Nunoue, InGaN light-emitting diodes on c-face sapphire substrates in green gap spectral range, Appl. Phys. Express 6 (11) (2013) 111004
- [2] P.T. Barletta, E.A. Berkman, B.F. Moody, N.A. El-Masry, A.M. Emara, M.J. Reed, S.M. Bedair, Development of green, yellow, and amber light emitting diodes using

- InGaN multiple quantum well structures, Appl. Phys. Lett. 90 (2007) 151109.
- [3] M.J. Reed, N.A. El-Masry, C.A. Parker, J.C. Roberts, S.M. Bedair, Critical layer thickness determination of GaN/InGaN/GaN double heterostructures, Appl. Phys. Lett. 77 (25) (2000) 4121–4123.
- [4] M.F. Schubert, S. Chhajed, J.K. Kim, E.F. Schubert, D.D. Koleske, M.H. Crawford, S.R. Lee, A.J. Fischer, G. Thaler, M.A. Banas, Effect of dislocation density on efficiency droop in GaInN/GaN light-emitting diodes, Appl. Phys. Lett. 91 (23) (2007) 231114.
- [5] Y.C. Shen, G.O. Mueller, S. Watanabe, N.F. Gardner, A. Munkholm, M.R. Krames, Auger recombination in InGaN measured by photoluminescence, Appl. Phys. Lett. 91 (14) (2007) 141101.
- [6] M. Maier, K. Köhler, M. Kunzer, W. Pletschen, J. Wagner, Reduced nonthermal rollover of wide-well GaInN light-emitting diodes, Appl. Phys. Lett. 94 (4) (2009) 41103
- [7] F. Scholz, et al., GaInN-based LED structures on selectively grown semi-polar crystal facets, Phys. Status Solidi (a) 207 (6) (2010) 1407–1413.
- [8] S.-H. Park, J. Park, E. Yoon, Optical gain in InGaN/GaN quantum well structures with embedded AlGaN δ layer, Appl. Phys. Lett. 90 (2) (2007) 23508.
- [9] S. Che, A. Yuki, H. Watanabe, Y. Ishitani, A. Yoshikawa, Fabrication of asymmetric GaN/InN/InGaN/GaN quantum-well light emitting diodes for reducing the quantum-confined stark effect in the blue-green region, Appl. Phys Express 2 (2) (2009) 21001
- [10] T. Ozaki, Y. Takagi, J. Nishinaka, M. Funato, Y. Kawakami, Metalorganic vapor phase epitaxy of GaN and lattice-matched InGaN on ScAlMgO4(0001) substrates, Appl. Phys Express 7 (9) (Aug. 2014) 91001.
- [11] J. Däubler, T. Passow, R. Aidam, K. Köhler, L. Kirste, M. Kunzer, J. Wagner, Long wavelength emitting GaInN quantum wells on metamorphic GaInN buffer layers with enlarged in-plane lattice parameter, Appl. Phys. Lett. 105 (2014) 111111.
- [12] K. Hestroffer, F. Wu, H. Li, C. Lund, S. Keller, J.S. Speck, U.K. Mishra, Relaxed c-plane InGaN layers for the growth of strain-reduced InGaN quantum wells, Semicond. Sci. Technol. 30 (2015) 105015.
- [13] T.L. Song, S.J. Chua, E.A. Fitzgerald, P. Chen, S. Tripathy, Characterization of graded InGaN/GaN epilayers grown on sapphire, J. Vac. Sci. Technol. A 22 (2) (2004) 287–292.
- [14] A. Even, G. Laval, O. Ledoux, P. Ferret, D. Sotta, E. Guiot, F. Levy, I.C. Robin, A. Dussaigne, Enhanced In incorporation in full InGaN heterostructure grown on relaxed InGaN pseudo-substrate, Appl. Phys. Lett. 110 (2017) 262103.
- [15] W.V. Lundin, et al., Single quantum well deep-green LEDs with buried InGaN/GaN short-period superlattice. J. Cryst. Growth 315 (1) (2011) 267–271.
- [16] N. Nanhui, et al., Enhanced luminescence of InGaN/GaN multiple quantum wells by strain reduction, Solid-State Electron. 51 (6) (2007) 860–864.
- [17] P.-C. Tsai, Y.-K. Su, W.-R. Chen, C.-Y. Huang, Enhanced luminescence efficiency of InGaN/GaN multiple quantum wells by a strain relief layer and proper si doping, Jpn. J. Appl. Phys. 49 (4S) (2010) pp. 04DG07.
- [18] Z.Y. Al Balushi, J.M. Redwing, In situ stress measurements during MOCVD growth of thick N-polar InGaN, J. Appl. Phys. 122 (8) (2017) 85303.
- [19] D.M. Van Den Broeck, D. Bharrat, Z. Liu, N.A. El-Masry, S.M. Bedair, Growth and characterization of high-quality, relaxed In_yGa_{1-y}N templates for optoelectronic applications, J. Electron. Mater. 44 (Nov 2015) 4161–4166.
- [20] D.M.V.D. Broeck, D. Bharrat, A.M. Hosalli, N.A. El-Masry, S.M. Bedair, Strain-balanced InGaN/GaN multiple quantum wells, Appl. Phys. Lett. 105 (2014) 031107.
- [21] K. Pantzas, et al., Semibulk InGaN: A novel approach for thick, single phase,

- epitaxial InGaN layers grown by MOVPE, J. Cryst. Growth 370 (2013) 57–62. [22] Y.E. Gmili, et al., Multilayered InGaN/GaN structure vs. single InGaN layer for solar
- cell applications: a comparative study, Acta Mater. 61 (17) (2013) 6587–6596.
 Z. Liliental-Weber, et al., Spontaneous stratification of InGaN layers and its influence on optical properties, Physica Status Solidi c 6 (S2) (2009) S433–S436.
- [24] Z. Liliental-Weber, D.F. Ogletree, K.M. Yu, M. Hawkridge, J.Z. Domagala, J. Bak-Misiuk, A.E. Berman, A. Emara, S. Bedair, Structural defects and cathodoluminescence of In_xGa_{1-x}N layers, Phys. Status Solidi (c) 8 (7–8) (2011) 2248–2250.
- [25] Z. Liliental-Weber, M. Benamara, J. Washburn, J.Z. Domagala, J. Bak-Misiuk, E.L. Piner, J.C. Roberts, S.M. Bedair, Strain relaxation of InGaN thin layers observed by X-ray and transmission electron microscopy studies, J. Electron. Mater. 30 (4) (Apr. 2001) 439–444.
- [26] Z. Liliental-Weber, K.M. Yu, M. Hawkridge, S. Bedair, A.E. Berman, A. Emara, D.R. Khanal, J. Wu, J. Domagala, J. Bak-Misiuk, Structural perfection of InGaN layers and its relation to photoluminescence, Phys. Status Solidi (c) 6 (12) (2009) 2626–2631
- [27] D. Holec, Y. Zhang, D.V.S. Rao, M.J. Kappers, C. McAleese, C.J. Humphreys, Equilibrium critical thickness for misfit dislocations in III-nitrides, J. Appl. Phys. 104 (12) (2008) 123514.
- [28] A.V. Lobanova, A.L. Kolesnikova, A.E. Romanov, S.Y. Karpov, M.E. Rudinsky, E.V. Yakovlev, Mechanism of stress strain relaxation in (0001) InGaN/GaN via formation of V-shaped dislocation half-loops, Appl. Phys. Lett. 103 (15) (2013) 152106.
- [29] J.E. Northrup, J. Neugebauer, Indium-induced changes in GaN(0001) surface morphology, Phys. Rev. B 60 (12) (Sep. 1999) R8473–R8476.
- [30] T.L. Song, Strain strain relaxation due to V-pit formation in InxGa1 xN/GaN epilayers grown on sapphire, J. Appl. Phys. 98 (8) (2005) 84906.
- [31] K. Watanabe, et al., Formation and structure of inverted hexagonal pyramid defects in multiple quantum wells InGaN/GaN, Appl. Phys. Lett. 82 (5) (2003) 718–720.
- [32] S. Pereira, M.R. Correia, E. Pereira, K.P. O'Donnell, E. Alves, A.D. Sequeira, N. Franco, I.M. Watson, C.J. Deatcher, Strain and composition distributions in wurtzite InGaN/GaN layers extracted from x-ray reciprocal space mapping, Appl. Phys. Lett. 80 (21) (2002) 3913–3915.
- [33] M.-I. Richard, et al., In situ synchrotron x-ray studies of strain and composition evolution during metal-organic chemical vapor deposition of InGaN, Appl. Phys. Lett. 96 (5) (2010) 51911.
- [34] G. Ju, M. Tabuchi, Y. Takeda, H. Amano, Role of threading dislocations in strain strain relaxation during GaInN growth monitored by real-time X-ray reflectivity, Appl. Phys. Lett. 110 (26) (2017) 262105.
- [35] M. Leyer, J. Stellmach, C. Meissner, M. Pristovsek, M. Kneissl, The critical thickness of InGaN on (0001)GaN, J. Cryst. Growth 310 (23) (2008) 4913–4915.
- [36] M. Schuster, et al., Determination of the chemical composition of distorted InGaN/ GaN heterostructures from x-ray diffraction data, J. Phys. D Appl. Phys. 32 (10A) (1999) A56.
- [37] A.M. Emara, E.A. Berkman, J. Zavada, N.A. El-Masry, S. Bedair, Strain strain relaxation in InxGa1-xN/GaN quantum well structures, Phys. Status Solidi c 8 (7–8) (2011) 2034–2037.
- [38] C.A. Parker, J.C. Roberts, S.M. Bedair, M.J. Reed, S.X. Liu, N.A. El-Masry, L.H. Robins, Optical band gap dependence on composition and thickness of $In_xGa_{1-x}N$ (0 < x < 0.25) grown on GaN, Appl. Phys. Lett. 75 (1999) 2566–2568.
- [39] J. Piprek, Nitride Semiconductor Devices: Principles and Simulation, John Wiley & Sons, 2007.